STIFFNESS EQUIVALENT SUBSTITUTION OF AN AIRFOIL PROFILE BY AN AUTOMATED MANUFACTURABLE CF/LM-PAEK TAILORED LAMINATE ARCHITECTURE

D. Laresser[1*], J. Birtha[1], E. Kobler[1], M. Binder[3], R. C. Adam[2], M. Gürocak[2], M.-C. Miron[1] and Z. Major[3]

[1] Competence Center CHASE GmbH, Altenberger Straße 69, 4040 Linz, Austria, daniel.laresser@chasecenter.at, www.chasecenter.at
[2] FACC Operations GmbH, Breitenaich 52, 4973 St. Martin im Innkreis, Austria, r.adam@facc.com, www.facc.com
[3] Johannes Kepler Universität Linz, Institute of Polymer Product Engineering, Science Park 2, Altenberger Straße 69, 4040 Linz, Austria, zoltan.major@jku.at, www.jku.at/ippe

Keywords: Thermoplastic composites, Tailored laminates, Automated processing, Design for automated manufacturing, Unidirectional tapes

ABSTRACT

Continuous fiber-reinforced thermoplastic composites, processable with high-rate automated manufacturing technologies, are gaining momentum in the aviation industry. In contrast to conservatively designed multilayer ply stacks of uniform thickness processed by stamp forming or hybrid molding, tailoring of laminates opens the door to weight/performance optimized and geometrically advanced components. However, automated layup methods have certain limitations that reduce the degree of freedom in laminate design. Therefore, this study addresses laminate design strategies *(BLOCK, CARD, CONV)* with the goal of stiffness equivalent substitution of an AL7075-T6 aluminum airfoil profile by a pick-and-place compliant architecture based on a CF/LM-PAEK unidirectional (UD) tape material and defined guidelines. In addition, stacked pure matrix films were incorporated as core layers in certain laminates (*THICK, THIN*) to capture the edge-filling behavior driven by squeeze flow during processing and its influence on mechanical performance and laminate quality. The tailored ply stacks were consolidated into a composite component using a two-stage consolidation unit with a specially designed tool insert and experimentally evaluated by means of a four-point bending test and digital microscopy. From a design point of view, this study has shown that by smart utilization of symmetry, fiber orientations, and ply dimensions, a realization of the airfoil profile shape within the limitations of the pick-and-place tape laying unit can be realized by a tailored architecture. Despite the challenging stiffness requirements, one architecture is presented that meets the defined requirements. With respect to the incorporation of neat matrix film core layers, it has been found that this approach does not significantly improve the edge filling behavior, results in a discontinuous distribution within the laminate, is prone to voids, and reduces mechanical performance.

1 INTRODUCTION

In thermoplastic composites, the aviation industry sees enormous potential for significant improvements in terms of sustainability and manufacturing cycles to meet production volumes for future mobility solutions. This drive is based on the material's ability to deform at high temperatures and solidify without chemical curing, which is an advantage over its thermoset counterparts. Automated high-rate process technologies and advanced material types are undergoing continuous development in this field [1, 2]. In stamp-forming or hybrid molding production processes, pre-consolidated multilayer ply stacks with uniform thickness based on thermoplastic unidirectional (UD) tapes or fabrics are predominantly used.

A common composite design approach, where fiber content, fiber orientations and stacking sequence are specified for defined load cases, results in a certain laminate thickness. To fully exploit the potential of composites in terms of weight/performance optimization, the thickness of a laminate can be adjusted by drop off plies in discrete steps, usually with respect to a prevailing stress condition. This concept is

referred to as tapering [3]. In addition, this concept shows potential to create discontinuous laminate cross-sections to meet shape requirements of a component, for example in areas relevant to air flow. Using laminate tailoring to achieve structural and geometric shape requirements only through layup architecture can reduce or eliminate milling and save resources.

However, the strive for an automated tape lay-up process is usually associated with technology-specific limitations in terms of the variety of prepreg shapes and contours that can be used for the laminate structure of a component. The consequence is a limited degree of freedom in the laminate design phase and a higher risk to fall short the demands of an advanced composite component. In other words, a complex tailored laminate architecture should be manufacturable under the limited variety of plies of an automated tape lay-up process by simultaneously fulfilling industry-specific guidelines, structural and shape requirements.

Motivated by these circumstances, this study addresses development strategies for laminate architectures tailored to a geometrically specified airfoil profile under the given manufacturing conditions of a pick-and-place tape laying cell (ENGEL Austria GmbH, Schwertberg, Austria). The objective is the bending stiffness-equivalent substitution of the aluminum AL7075-T6 counterpart of the component by a laminate architecture based on thermoplastic CF/LM-PAEK UD tapes. Three laminate design approaches are presented, corresponding layups manufactured, and composite components produced with a specific mold insert on a consolidation unit under a deliberately chosen high-rate process cycle of eight minutes. In addition, one architecture is modified by substitution of core plies with pure LM-PAEK polymer films to investigate the resulting influence on the mechanical performance, laminate quality, and filling behaviour of the components filigree edge sections.

The structural mechanical performance of the composite components is evaluated experimentally using a four-point bending load case, while the AL7075-T6 benchmark is determined by a finite element simulation model. To assess the laminate quality under the given design and process conditions, cross-section specimens are examined using digital microscopy.

2 MATERIALS AND GEOMETRY

For this study, the commercially available thermoplastic UD tape Toray Cetex® TC1225 is used. It has a density of 1.3 g/cm³ and is composed of a low-melt polyaryletherketone (LM-PAEK) polymer with a melting point of 305 °C, reinforced with continuous standard modulus carbon fibers with a volume content of 59 % [4]. Based on own measurements on consolidated multilayer panels, the nominal consolidated ply thickness is set to t_{ply} = 0.136 mm for the purpose of laminate architecture development in this study. The neat polymer LM-PAEK film used is Victrex APTIV AE™ 6013-AEG-060 with a nominal thickness of t_{film} = 0.060 mm.

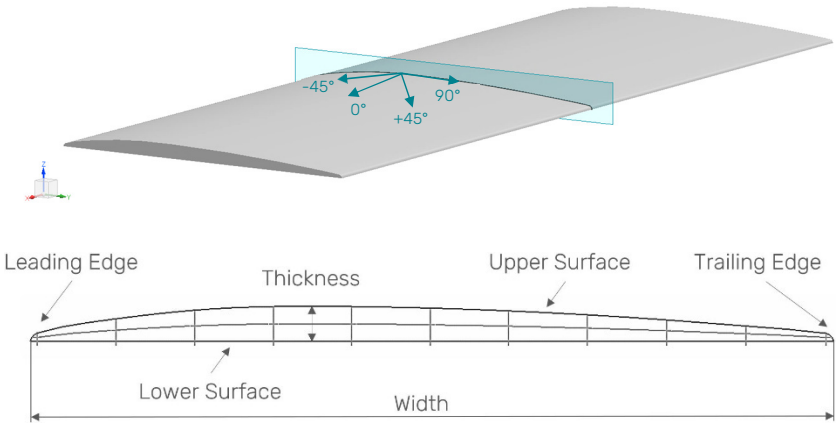

Figure 1: Geometry of the airfoil profile (top) and cross-section details (bottom).

Fig. 1. shows the used research geometry which is derived from a commercial component considering specific measurements. The geometric characteristics include a width of w = 78 mm, a maximum

thickness of t_{max} = 3.46 mm, radii of less than 1 mm at the leading and trailing edge, a curved upper surface, and a flat lower surface. The cross-sectional area amounts to A = 197.15 mm² and the length of the profile is defined to l = 220 mm.

3 DEVELOPMENT OF LAMINATE ARCHITECTURES

This section presents three approaches that address the realisation of tailored laminate architectures for the given geometry. The literature provides several guidelines for designing tapered zones to merge adjacent laminates in a manner that optimizes structural integrity for load transfer [3, 5, 6]. However, given geometric boundary conditions and material type will determine the applicability of these guidelines. This means that, at best, a designer can use guidelines to a maximum extent and may not use them holistically. The basic design guidelines followed for this stand-alone laminate component and the constraints imposed by pick-and-place tape laying are summarized in Table 1. Based on that, a two-step iterative development strategy was used for layup development. First, the focus was on the elaboration of stacking solutions to meet the geometry requirement, followed by the definition of the fiber orientations. To reduce the complexity in the design process and in future numerical investigations, layers were double stacked whenever possible. Since drop-off laminate designs can be prone to local asymmetries and guidelines are not always enforceable [6], the local laminate structure at the thickest component position (t_{max}) is used as a reference for the guidelines 2-4 (see Table 1).

	Automated pick-and-place tape laying restrictions			
R1	Maximum number of individual ply contours		-	6
R2	Minimum ply width to handle		mm	25
	Laminate design guidelines			
1	QUAD	Using at least four distinct ply angles (0°, 90, +45°, -45°; as usual in aerospace)		[5, 6]
2	10%-rule	At least 10% of plies oriented at each angle (Better accommodation of secondary loads and reduction of matrix-dominant properties, e.g. creeping)		[5, 6]
3	Symmetry	Stacking sequence symmetric about the midplane (Avoids extension-bending coupling)		[5, 6]
4	Balancing	Equal numbers of plies with +θ and -θ fiber orientation (Avoids shear-extension coupling)		[5, 6]
5	Cover plies	Covering continuous layer on the bottom and top surface (Reduce the risk of edge delamination at drop-offs)		[6]
6	± 45° cover layer	Using cover plies with fiber orientation of ±45° (Improves damage tolerance, impact and buckling resistance)		[6, 7]

Table 1: Restrictions and guidelines considered best possible in laminate architecture development.

3.1 Laminate architectures

This subsection briefly describes the strategies used to develop the three laminate architectures and presents the resulting layups that were fabricated and tested.

3.1.1 Blocking (BLOCK)

In this approach, the initial cross-section (see Fig. 1, bottom) was alternately sliced from the top and bottom in offset steps of $2 \cdot t_{Ply}$ = 0.276 mm, and the mid-surfaces and their flat patterns were generated from the resulting sections. Based on the geometric analysis of the flat layer structure, those layers with similar widths were grouped together, with the width of a group being the average of its layers. After

assigning fiber orientations to the groups, the resulting preliminary layup was subjected to an iterative refinement process, in which the width of the ply groups and the horizontal position of the plies were optimized. Care was taken to ensure that the total width of the 0° plies was realized as a multiple of narrower 0° plies with a minimum width of 25 mm placed in parallel as a method to reduce the total amount of individual ply widths. As an additional step, the middle layer was extended to a continuous layer, which seems advantageous from a design point of view in terms of a convenient measure for thickness adjustment for this type of architecture, while maintaining the mechanical characteristic of the laminate. The final architecture *BLOCK,* with reference to the initial cross-sectional cut (Fig. 1, bottom), is shown in Fig. 2.

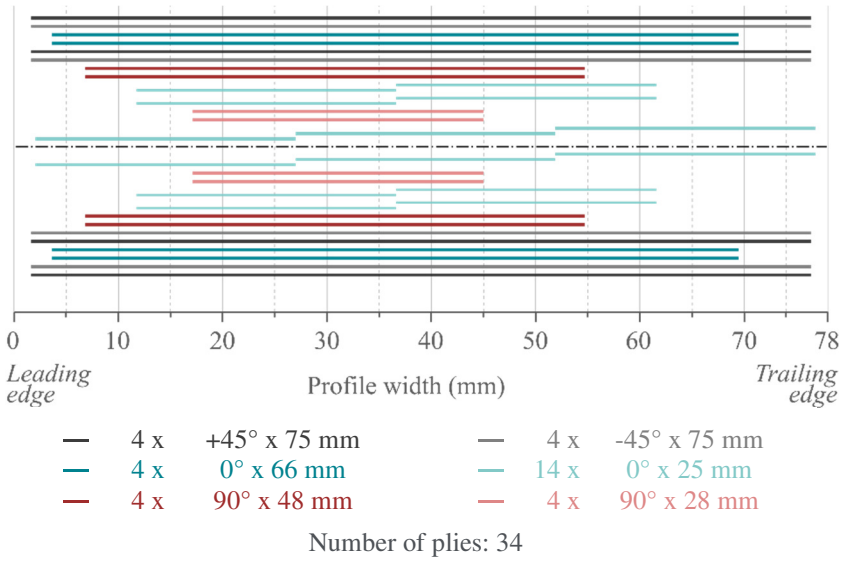

Figure 2: Laminate architecture *BLOCK*.

3.1.2 Card Sliding (CARD)

This approach is inspired by the “card sliding” technique proposed by Tsai [8]. Based on the available internal space, limited by four cover plies each at the top and bottom, a possible laminate structure according to “card sliding” was first estimated by two blocks of sliding layers following the curvature of the outer surface of the profile, starting from the side of the trailing edge. Due to the non-symmetric cross-section and the discontinuous slope of the outer surface, the layup exhibits a deflection edge and requires the incorporation of compensation layers to fill the area on the side of the leading edge. Fiber orientations and final ply widths were defined in a final refinement step, taking care to realize the 0° layers, including the compensation layers, by parallel placement of two narrower 0° plies. The final architecture *CARD* is shown in Fig. 3.

3.1.3 Conventional (CONV)

This approach starts with six predefined layer widths of 77, 70, 60, 50, 40 and 30 mm. By stacking laterally offset layers of equal width from bottom to top, the cross-sectional shape was filled. The 60 mm and 30 mm layers were assigned a fiber orientation of 0° to replace the larger layer with two 30 mm layers. The resulting architecture can be seen in Figure 4.

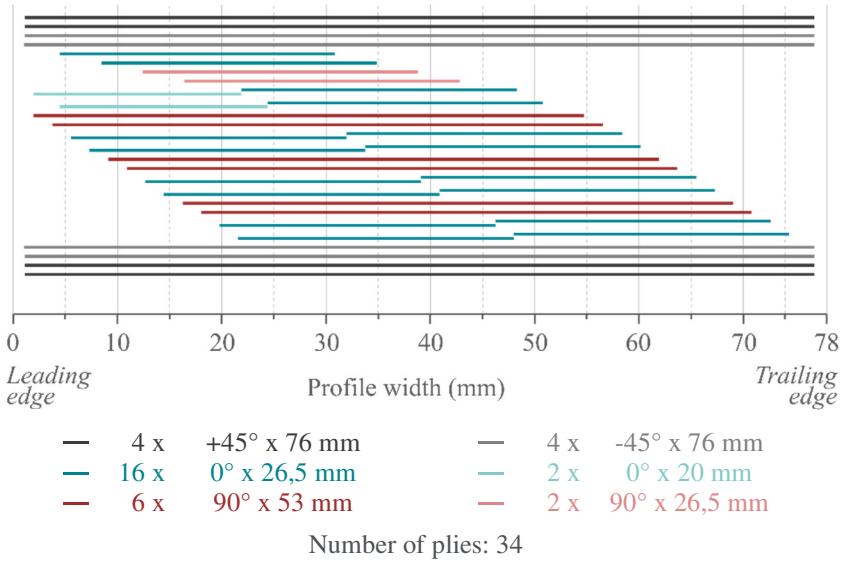

Figure 3: Laminate architecture *CARD*.

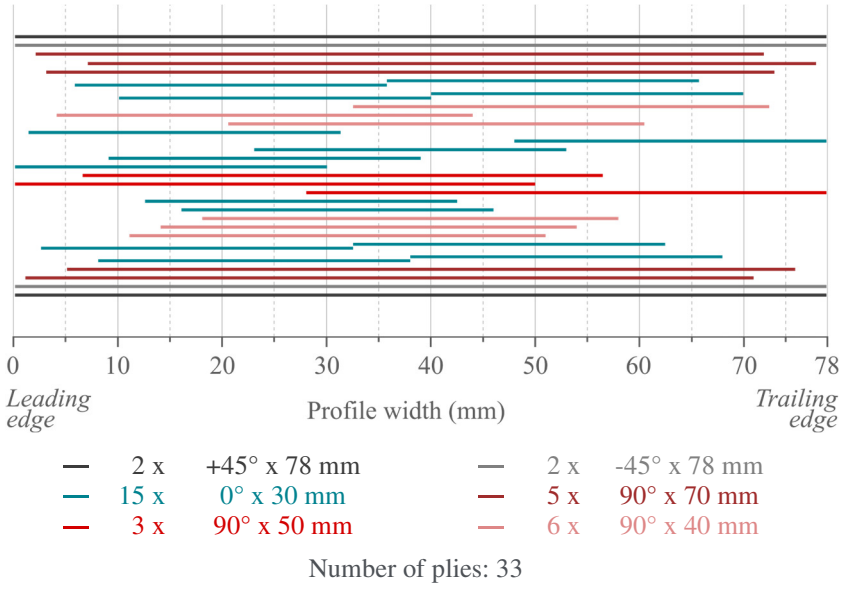

Figure 4: Laminate architecture *CONV*.

3.1.4 Polymer film modifications (REF, THIN, THICK)

In addition to the three laminate architectures presented above, modifications were made based on the *CONV* architecture, by replacing the core layers with pure polymer films. The aim was to determine whether matrix squeeze flow during processing positively affects the filling behavior of the component edges and how the resulting polymer core affects mechanical performance or laminate quality. In addition, the fiber orientation of the cover layers was changed from ±45° to 0°, referred to as reference configuration *REF*. The designation *THIN* refers to the modification in which the middle 90° layers were replaced (Fig. 5 (a)), and THICK refers to the modification in which the adjacent 0° layers were also replaced by double stacked pure polymer films (Fig. 5 (b)).

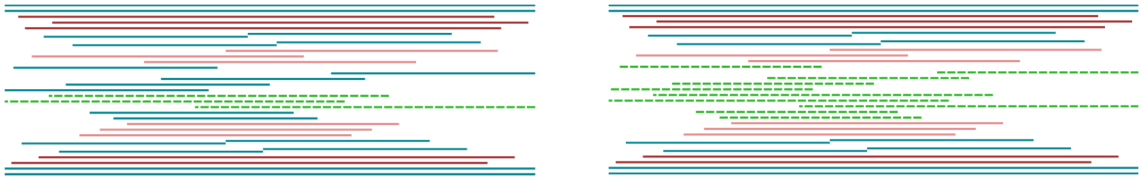

(a) (b)

Figure 5: Modifications *THIN* (a) and *THICK* (b) with polymer film core layers based on *CONV*.

4 EXPERIMENTAL

This chapter presents the experimental methods used to produce and test the laminate architectures and the FE simulation model used to determine the stiffness response of the AL7075-T6 reference component.

4.1 Composite component manufacturing

Since the test scope includes several types of ply stacks and a small number of total stacks, they were laid by hand using length gauges according to the architectures presented above. Individual cut tapes were spot-welded with a soldering iron to fix them in place. Consolidation of the tailored ply stacks took place at the LIT Factory (Linz, Austria) with a two-stage consolidation unit (FILL GmbH, Gurten, Austria), consisting essentially of a heating press, a cooling press and a shuttle system. For the airfoil geometry, a specific mold insert made of steel was implemented and positioned between the carrier tool plates, as shown in Fig. 6. A small strip of polyimide sticky tape was attached to each end section of the ply stacks to hold them in place as positioned during mould closing.

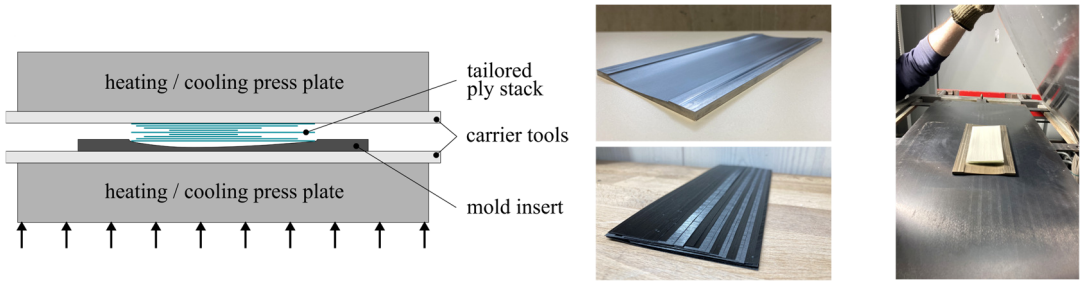

(a) (b) (c)

Figure 6: Consolidation of tailored ply stacks: Illustration of the consolidation setup (a), mold insert and ply stack (without cover plies) (b), manufacturing unit (c)

To ensure a consolidation temperature of 365 °C within a deliberately chosen fast process cycle, preliminary tests were conducted on laminate stacks with incorporated thermocouples. The process parameter used in this study can be seen in Table 2.

Process parameter	Unit	Heating press	Cooling press
Temperature	°C	365	100
Pressure	bar	4.1	10.0
Time	min	4	4

Table 2: Process parameter set of rapid ply stack consolidation cycle.

4.2 Four-point bending component testing

Experimental evaluation of the mechanical performance of the laminate architectures was performed according to a four-point bending test oriented on the ASTM D6272 standard. As testing environment served the servo-hydraulic testing machine MTS 852 (MTS Systems Corporation, USA), equipped with a 50 kN load cell and a custom four-point bending setup with a support span length of 164 mm, a load span length of 78 mm, and nose radii of 15 mm. The setup is shown in Fig. 7. All tests were conducted at room temperature and at a test speed of 10 mm/min. Three components were tested for each laminate architecture.

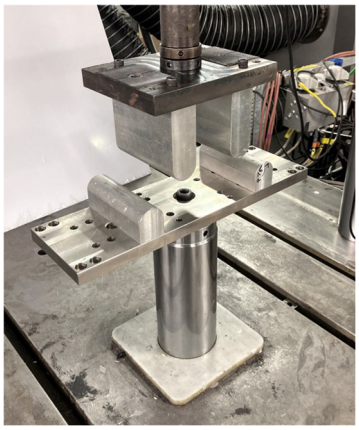

Figure 7: Four-point bending test setup.

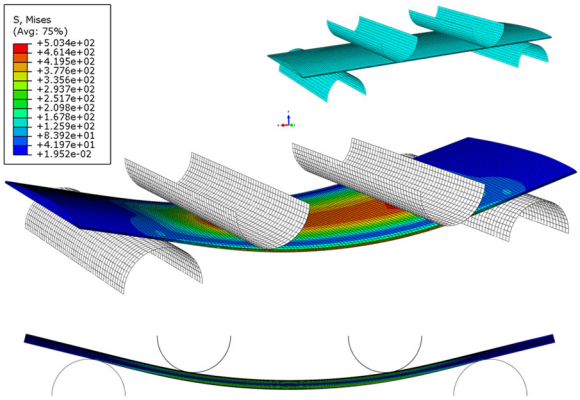

Figure 8: FE simulation model.

4.3 FE simulation

To determine the mechanical response of the reference part made of AL7075-T6, a finite element (FE) simulation according to the experimental four-point bending setup was performed in ABAQUS/Standard (SIMULIA, Dassault Systems). The supports and loading noses were discretized by rigid shell elements of type R3D4 with a mesh size of 2 mm. Discretization of the component followed by 5 uniformly distributed solid hexa elements of type C3D8R through the thickness with an approximate global mesh size of 1.5 mm and a refined mesh density at the leading and trailing edges. The contacts between specimen and supports or specimen and loading noses were modelled by the surface-to-surface formulation with a coefficient of friction of 0.2. To conveniently extract the resulting reaction force data, a reference point was coupled to the loading noses. An illustration of the FE model is given by Fig. 8 and the applied material properties are summarized in Table 3.

Property	Unit	Value
E-Modulus	GPa	72
Poisson's ratio	-	0.33
Yield stress	MPa	505
Density	g/cm³	2.81

Table 3: Material properties of AL7075-T6 [9] used for the FE model.

4.4 Digital microscopy

For evaluation of the internal laminate structures, 15 mm wide cross-sectional specimens were milled from the center of each laminate architecture and prepared with sandpaper for digital microscopy. Fig.

9 illustrates where the specimens were taken from the composite components and shows one representing the *CARD* architecture.

Figure 9: Position of cross-sectional specimens for microscopy.

5 RESULTS AND DISCUSSION

This section presents the results of the experimental evaluation of the mechanical performance under a four-point bending load scenario and the quality of the designed and fabricated laminate architectures.

5.1 Mechanical performance of the composite components

The measured force-deflection results including the AL7075-T6 benchmark curve determined by simulation are presented in Fig. 10, where (a) refers to the *BLOCK*, *CONV*, *CARD* laminates and (b) refers to *REF* with the polymer core layer variants *THICK* and *THIN*. The curves are given as the average of $n = 3$ components tested to the point of ultimate load.

All experimental curves show similar characteristics, with a region of linear behavior exhibiting after a nonlinear initial region, and a decrease in stiffness signaling the occurrence of the maximum tolerable load. This nonlinear initial behavior, known as the toe region, can be an artifact caused by alignment and seating of the sample during the initial phase of the test procedure, which superimposes the true response in this region [10]. A general compensation for the toe region, as suggested in [10], was not applied to the data. Since this effect is less pronounced for the components with 0° cover layers (Fig. 9 (b)), this implies that a portion of the nonlinear initial response is rooted in the ±45° cover layers. The component stiffnesses used for evaluation, which correspond to the slope of the force-deflection curves, were derived from a linear fit of the linear region shown as thin dotted lines in the diagrams.

The reference stiffness value of the aluminum component was taken from the linearized initial range of the simulation up to the deflection of 3 mm.

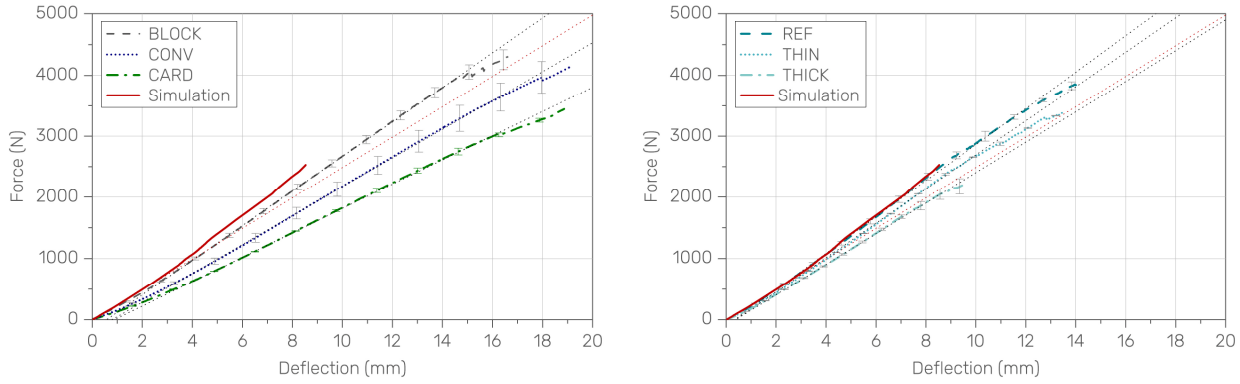

(a) (b)

Figure 10: Force-deflection curves of four-point bending testing the composite components with (a) *BLOCK, CONV, CARD* laminate architectures and (b) *REF* architecture and its adaptions with *THICK* and *THIN* polymer core layers.

As derived from the experimental curves, Fig. 11 shows the achieved component stiffnesses (a) and

strengths (b) of the different laminate architectures, with the corresponding data summarized in Table 4. With respect to the ±45° cover layer architectures, *BLOCK* outperformed both *CONV* and *CARD* in terms of stiffness and strength. Only *BLOCK* was able to meet the benchmark in terms of component stiffness. For the test set with 0° cover layers and polymer core layers, it can be seen that the incorporated films lead to a decrease in stiffness and significantly weaken the structure in terms of strength.

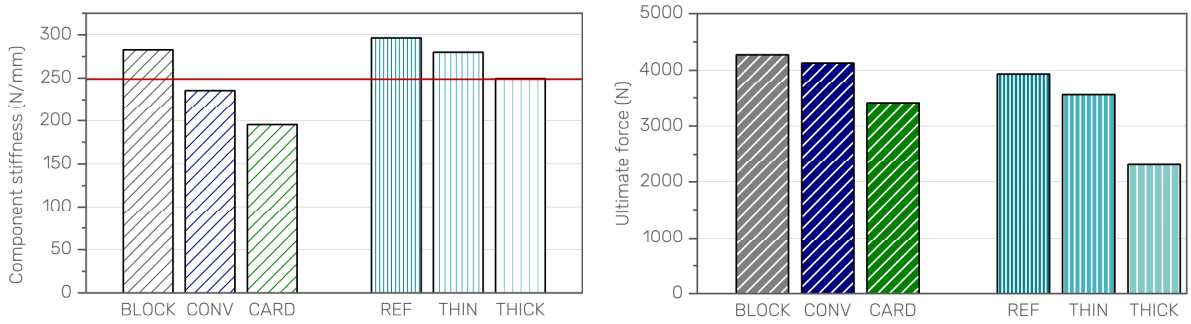

(a) (b)

Figure 11: Comparison of component stiffness (a) and ultimate force (b) of the different laminate architectures.

Laminate architecture	Bending stiffness (N/mm)	Ultimate load (N)
BLOCK	282.9	4273.2
CONV	235.9	4130.9
CARD	195.3	3406.1
REF	296.5	3934.2
THICK	280.2	3555.6
THIN	249.8	2305.3

Table 4: Summary of experimentally determined characteristics.

5.2 Laminate quality

To draw inferences about the quality of the internal laminate structures, characteristic features of the laminate architectures were gathered by cross-sectional microscopy of specimens taken from the center of the components (Fig. 9). Selected representative images are presented in Fig. 12.

From a geometric point of view, all architectures were able to reproduce the desired shape of the discontinuous cross-section and properly form the filigree edge sections, as can be seen in Fig. 12 (left column). The findings are identical for the opposing trailing edge side of the component. The *BLOCK* and *CARD* architectures (Fig. 12 (a)-(d)) embody a defined laminate structure and ply alignment compared to *REF* and the *THICK* and *THIN* modifications, which exhibit a more pronounced ply waviness and irregular structure through the thickness. Fig. 12 (g) and (i) indicate that the filling of the edge areas is achieved by the squeeze flow of the UD tape material rather than by the pure polymer material incorporated in the center. The polymer film approaches resulted in laminates with discontinuously distributed polymer cores and were prone to voids in both the polymer core and the surrounding laminate structure (Fig. 12 (g)-(j)). However, a positive effect of the neat polymer on corner filling behavior around terminated plies was noted (Fig. 12 (j)). Voids related to ply drop-off pockets, as shown in Fig. 12 (f), were detected in varying numbers in all laminate architectures, however, measuring the void content to quantify the consolidation quality of each laminate architecture was not within the scope of the present work.

While *BLOCK* or *CARD* and the omission of multilayer polymer film emerged as favorable design strategies for nearly "as-designed" manufacturable laminate structures with respect to the geometry under investigation, process- and tooling-related optimizations are seen as quality-enhancing measures to bring laminate quality towards aerospace standards.

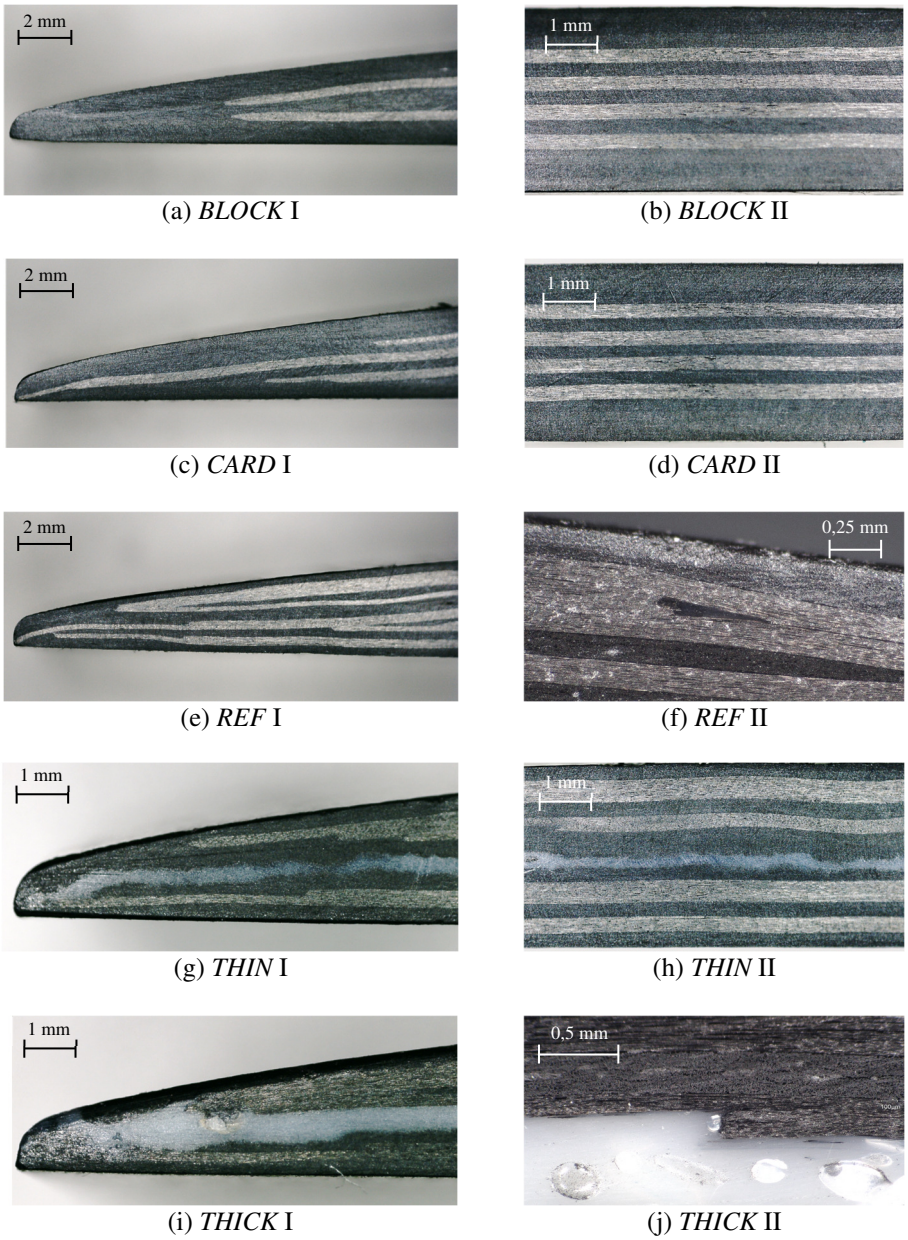

(a) *BLOCK* I (b) *BLOCK* II

(c) *CARD* I (d) *CARD* II

(e) *REF* I (f) *REF* II

(g) *THIN* I (h) *THIN* II

(i) *THICK* I (j) *THICK* II

Figure 12: Microscope cross-sectional images.

6 CONCLUSIONS

This study addressed strategies for tailored laminate architectures based on CF/LM-PAEK thermoplastic UD tapes to replace an AL7075-T6 aluminum airfoil profile in terms of bending stiffness equivalence and under specific design constraints. These comprised (i) a maximum number of different ply geometries of six and (ii) a minimum ply width of 25 mm, as well as industry-specific guidelines. Three different strategies and two additional modifications using a polymer core by replacing plies with stacked neat polymer films are presented.

One approach, named *BLOCK*, was identified as having the most potential in terms of automated manufacturability, mechanical performance, compliance with industry guidelines, flexibility for modification, and, in summary, substitution of the aluminum component. From the components with polymer core layer, it can be concluded that this strategy is not crucial to significantly improve the mold filling of the filigree edge sections. Rather, the multilayer polymer core exhibits adverse effects such as pores, discontinuous propagation, and, especially as the core becomes thicker, a significant reduction in mechanical strength. However, the polymer shows a positive filling effect in the areas of discrete ply steps, suggesting a possible useful local application at ply drop-off regions.

Certain imperfections in the laminate architectures detected by microscopy lead to the conclusion that the laminate quality achieved under the applied rapid processing conditions does not meet aerospace standards. In addition, the cooling rate in part production was higher than otherwise optimal for this material due to the low cooling press temperature. Measurements to determine the direct effect on the final crystallinity level were not performed within this study. However, given the focus of this work on design strategies and the fact that the final quality of a composite part is an interaction of design, material and process, an improvement in quality and component performance is seen through optimized processing and tooling. Considering the types of aluminum and thermoplastic composite used in this work, the weight saving potential is approximately 54% in terms of material substitution.

ACKNOWLEDGEMENTS

This work was performed within the Competence Center CHASE GmbH, funded by the Austrian Research and Promotion Agency. The authors acknowledge financial support by the COMET Centre CHASE, which is funded within the framework of COMET—Competence Centers for Excellent Technologies—by BMVIT, BMDW, and the Federal Provinces of Upper Austria and Vienna. The COMET program is run by the Austrian Research Promotion Agency (FFG).

REFERENCES

[1] J. Sloan, *I want to say two words to you: Thermoplastic tapes*, Composites World [Online], Available:https://www.compositesworld.com/articles/i-want-to-say-two-words-to-you-thermoplastic-tapes, [Accessed 16 10 2022].

[2] B. Y. Zeyrek, B. Aydogan, E. Dilekcan, and F. Ozturk, Review of Thermoplastic Composites in Aerospace Industry, *International Journal on Engineering Technologies and Informatics*, **3** (1), 2022, pp. 1-6 (doi: 10.51626/ijeti.2022.03.00031).

[3] A. Mukherjee and B. Varughese, Design guidelines for ply drop-off in laminated composite structures, *Composites: Part B*, **32**, 2021, pp. 153-164 (doi:10.1016/S1359-8368(00)00038-X)

[4] Toray Advanced Composites (CA, USA), *Product Data Sheet: Toray Cetex® TC1225*, TC1225_PDS_v4.1_2020-04-22

[5] US Department of Defense, *Composite Materials Handbook*, MIL-HDBK-17-3F, Vol. 3, 2002.

[6] J.A. Bailie, R.P. Ley and A. Pasricha. *A summary and review of composite laminate design guidelines*. Technical report NASA, NAS1-19347. Northrop Grumman Military Aircraft Systems Division, 1997

[7] G. Jogur, A. Nawaz Khan, A. Das, P. Mahajan and R. Alagirusamy, Impact properties of thermoplastic composites, *Textile Progress*, **50** (3), 2018, pp. 109-183 (doi: 10.1080/00405167.2018.1563369)

[8] S.W. Tsai, Double-double: New family of composite laminates, *AIAA Journal*, **59** (11), 2021

[9] Metals Handbook, *Properties and Selection: Nonferrous Alloys and Special-Purpose Materials*, Vol. 2, ASM International, 1990.

[10] ASTM Standard D 6272. *Flexural Properties of Unreinforced and Reinforced Plastics and Electrical Insulating Materials by Four-Point Bending*. ASTM International, West Conshohocken, PA, 2002.